Journal of Science, Innovation and Creativity
Vol. 5 No. 1 (2026): ISSN (Online): 2958-454X
DOI: https://doi.org/10.58721/jsic.v5i1.1705
Numerical Analysis of Magnetohydrodynamics Hybrid Nanofluid Flow Past an Infinite Vertical Plate in Presence of Thermal Radiation

Numerical Analysis of Magnetohydrodynamics Hybrid Nanofluid Flow Past an Infinite Vertical Plate in Presence of Thermal Radiation

Eva Chepkirui[1] & Maurine Wafula[2]
[1]*Kenyatta University, Kenya*
[2]*United States International University – Africa, Kenya*

Article History
Received: 2026-01-06
Revised: 2026-05-10
Accepted: 2026-05-12
Published: 2026-05-17

Keywords
Hybrid nanofluid
Magnetohydrodynamic flow
Nusselt number
Thermal radiation

How to cite:
Chepkirui, E., & Wafula, M. (2026). Numerical Analysis of Magnetohydrodynamics Hybrid Nanofluid Flow Past an Infinite Vertical Plate in Presence of Thermal Radiation. *Journal Science, Innovation and Creativity, 5*(1), 97-116.

Abstract
This study investigates magnetohydrodynamic (MHD) flow and heat transfer of a Cu–Al_2O_3/water hybrid nanofluid past an infinitely vertical plate, motivated by applications in energy generation, industrial cooling, and biomedical systems. Governing equations were reduced via similarity transformations and solved numerically using the shooting method with a fourth-order Runge–Kutta scheme in MATLAB. Results show that buoyancy and radiation parameters accelerate the boundary-layer flow, increasing skin friction and Nusselt number, while stronger magnetic fields suppress velocity due to Lorentz damping. Higher Prandtl numbers enhance heat transfer but thin the thermal boundary layer, reducing wall shear. Radiation decreases the Nusselt number yet increases skin friction, while nanoparticle volume fraction strengthens temperature fields. Entropy generation analysis highlights the competing roles of viscous dissipation and heat transfer irreversibility. Magnetic and Brinkman numbers intensify entropy production and weaken thermodynamic efficiency, whereas the temperature-difference parameter reduces entropy generation and raises the Bejan number. Radiation elevates both entropy generation and Bejan number. Comparative evaluation shows Cu–water producing the highest entropy generation, Al_2O_3–water the lowest, and the hybrid nanofluid maintaining intermediate values, demonstrating balanced thermal conductivity and viscosity. The hybrid nanofluid offers a balanced performance, improving heat transfer while limiting entropy generation, and thus holds promise for efficient energy utilisation in magnetohydrodynamic and radiative systems.

Introduction

In recent years, science and technology have played a vital role in power generation, the pharmaceutical industries, applications in medicine, refrigeration, and heating. The systems will depend on good thermal management systems for these industries to operate effectively and functionally. Various studies have been conducted to overcome the challenges caused by the low thermal conductivities of these fluids. Maxwell (1873) proposed adding millimetre-sized particles to a fluid. The results showed that there was a better thermal conductivity than ordinary fluids. This prompted Choi and Eastman (1995) to introduce nanometer-sized solid particles in place of millimetre-scale solid particles (with dimensions between 1 and 100 nanometers) dispersed

throughout a base fluid, which includes liquids like ethylene glycol, water, and oil. The nanometer-sized particle was later named a nanoparticle. The resulting suspension of nanoparticles in a base fluid is coined as nanofluids. These fluids exhibit enhanced heat transfer properties and thermal conductivity. Nanofluids have been successfully utilised in various applications, including cooling systems, electrical devices, nuclear reactors, the biomedical field, and automotive devices. The vast applications of nanofluids have sparked the curiosity in research as to whether there is a fluid with better conductivity as compared to nanofluids, leading to the discovery of hybrid nanofluid, which is a specialised group of nanofluids that is obtained by distributing many types of nanoscale particles into a base fluid. This was investigated by Hayat and Nadeem (2017). Using a specific material may not have the required properties needed for certain applications; hence, the right choice of nanoparticles and concentration can be optimised to achieve the desired thermal conductivities, heat transfer, and viscosity. Shoaib et al. (2020) demonstrated that hybrid nanofluids prepared by dispersing silver (Ag) and aluminium oxide (Al_2O_3) nanoparticles in water exhibited superior thermal conductivity compared to single-particle nanofluids. Hybrid nanofluids are useful in improving heat transmission in thermal systems compared to conventional fluids. Waini et al. (2020b) focused on the mixed convection flow and heat transfer of a Cu–Al_2O_3/water hybrid nanofluid over exponentially stretching and shrinking vertical surfaces, examining how nanoparticles enhance heat transfer, how suction reduces it in shrinking cases, and how bifurcated solutions behave under stability analysis. Amran et al. (2024) reviewed mixed convection heat transfer across fluids with varying Prandtl numbers and geometries. Manimaran et al. (2025) examined water-based hybrid nanofluids, stressing thermal conductivity and stability. Khalatbari et al. (2025) investigated hybrid nanofluids through experimental, numerical, and analytical approaches, reporting up to 35% improvement in heat transfer. Further research on hybrid nanofluids includes (Hafeez et al. 2025; Molla et al. 2025; Nayak et al., 2025).

The presence of magnetohydrodynamics in hybrid nanofluid has been shown to be of great significance in electricity generation, cooling systems, geophysics, optical fibres, and magneto-optical fibre wavelength sensors. Younes et al. (2015) scrutinised the thermal analysis of nanofluids in the presence of magnetic fields. Krishna et al. (2021) studied the magnetohydrodynamics stream of Casson hybrid nanofluid past a porous vertical medium. Suresh et al. (2023) studied magnetohydrodynamics Casson nanofluids and incorporated factors such as activation energy, Hall current, and thermal radiation. Mahdy et al. (2021) analysed magnetohydrodynamics stream of micropolar hybrid nanofluids past a permeable perpendicular medium. Nayak et al. (2017) examined three-dimensional magnetohydrodynamics flow of nanofluids past a porous linearly lengthening sheet. Ullah et al. (2021) focused on computational modelling of magnetohydrodynamics hybrid nanofluid motion over a stretchable surface. Further, Waini et al. (2020a) focused on analysing the magnetohydrodynamic flow and heat transfer of a Cu–Al_2O_3/water hybrid nanofluid over an exponentially shrinking sheet, incorporating radiation effects and dual solution stability.

Thermal radiation refers to the transfer of energy through electromagnetic waves. This mode of heat transfer does not rely on the presence of a material medium, making it distinct from conduction and convection. It is a technique of controlling excessive heat emission. Thermal radiation has wide applications in solar energy, satellites, missiles, atomic power plants, and microwave ovens (Xuan, 2014). Anantha (2020) studied the heat transfer of Casson fluids with thermal radiation. Daniel et al. (2019) scrutinised heat radiation on a wavy magnetohydrodynamics stream of nanofluids past an expanding surface, considering chemical reaction effect, and concluded that the existence of magnetism and suction force decelerates fluid movement, but higher values of electric field escalate

the movement, creating a sticky effect. The increase in thermal radiation stimulates the energy of the nanofluid. Brownian movement and discontinuity parameter result in an increase in the Nusselt number. Reddy and Goud (2023) researched the impact of ramped temperature and electromagnetic waves on a wavy magnetohydrodynamics nanofluid flow. Mohanty et al. (2015) examined thermal and mass exchange of micropolar hybrid nanofluids past an expanding sheet. Daniel et al. (2017) investigated joule heating and viscous dissipation with thermal radiation. Rajesh and Chamkha (2022) analysed the effect of a hybrid nanofluid stream on unsteady magnetohydrodynamics and heat transfer. Nath and Deka (2024) scrutinised how wavy magnetohydrodynamic nanofluid flow across an exponentially driven, permeable vertical surface is affected by temperature and mass stratification. Sheikholeslami et al. (2015) analysed the impact of thermal energy on fluid stream and heat transmission of magnetohydrodynamic nanofluids by incorporating a two-phase model. Alharbi et al. (2019) investigated thermal analysis of hybrid nanofluid containing Aluminium Oxide as a single type of nanoparticle and a combination of Aluminium Oxide and Copper as nanoparticles dispersed in a tangent hyperbolic fluid. Yashkun et al. (2021) examined MHD hybrid nanofluid flow over linearly deforming surfaces with suction and radiation, showing that Cu–Al_2O_3/water hybrids enhance heat transfer while radiation reduces the Nusselt number, results that align with the present study.

Despite extensive studies on MHD hybrid nanofluid flows with thermal radiation, most investigations have concentrated on first-law quantities such as velocity, temperature, skin friction, and the Nusselt number. While these parameters describe transport rates, they do not capture energy losses within the system. To address this limitation, the present study incorporates a second-law analysis based on entropy generation. Irreversibility in the flow arises from thermal gradients, viscous effects, and magnetic field interactions, all of which contribute to energy degradation. Entropy generation provides a quantitative measure of these losses, while the Bejan number identifies whether heat transfer or fluid friction dominates the irreversibility, following the thermodynamic framework established by Bejan & Kestin (1983). Although this approach has been applied in MHD and nanofluid studies (Murugan et al., 2024; Sharma et al., 2024; Rangra et al., 2025), its application to hybrid nanofluid flow over a vertical plate with simultaneous magnetic and radiative effects remains comparatively limited. In particular, the combined impact of hybrid nanoparticle interactions, magnetic forces, and thermal radiation on irreversibility has not been sufficiently examined within a unified framework.

This study extends existing models by analysing MHD hybrid nanofluid flow over a vertical plate using a Cu–Al_2O_3/water mixture. The effects of magnetic field strength, thermal radiation, and nanoparticle concentration are investigated. In addition to conventional transport quantities such as the Nusselt number and skin friction coefficient, entropy generation and the Bejan number are employed to assess thermodynamic irreversibility within the boundary layer. Importantly, the analysis compares Cu–water, Al_2O_3–water, and Cu–Al_2O_3/water hybrid nanofluids to reveal how each fluid influences entropy generation and Bejan number, an aspect often overlooked in earlier studies. This provides a more complete evaluation of system performance, with relevance to solar thermal systems, biomedical heat transfer, and industrial processes.

Novelty of the Study

- The work integrates first-law quantities (velocity, temperature, skin friction, Nusselt number) with second-law measures (entropy generation and Bejan number) to provide a comprehensive performance evaluation.

- It systematically compares Cu–water, Al_2O_3–water, and Cu–Al_2O_3/water hybrid nanofluids, showing their distinct impacts on entropy generation and Bejan number, which most studies do not address.
- It examines the combined effects of magnetic field strength, thermal radiation, and nanoparticle concentration on boundary-layer irreversibility within a unified framework.
- It links the findings to practical applications in solar energy, biomedical cooling, and industrial heat management, demonstrating the relevance of hybrid nanofluid optimisation to real engineering challenges.

Model formulation

A laminar, two-dimensional, steady, incompressible flow of magnetohydrodynamics hybrid nanofluid past an infinitely long vertical plate in the existence of thermal radiation with magnetic field intensity (B_0) acting transversely is considered. The fluid moves across an infinitely long vertical surface aligned in the (x)-direction and the no-slip condition is considered as shown in (Figure 1). The equations employed in this study are formulated on the basis of established models and previously validated approaches, ensuring alignment with the broader hybrid nanofluid literature. The governing relations for hybrid nanofluid flow are presented here in accordance with the methodologies reported by Waini et al. (2020).

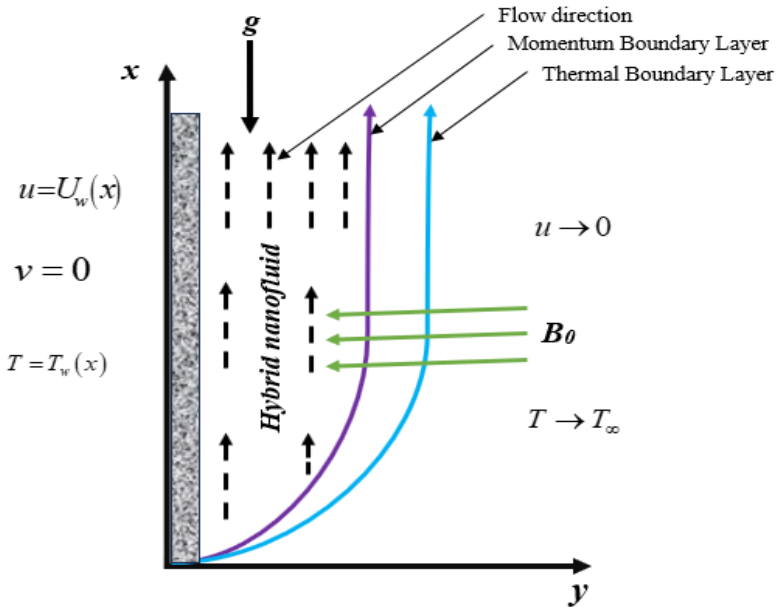

Figure 1: Schematic flow diagram of the hybrid nanofluid with magnetic field strength(B_0) acting in a perpendicular direction

$$\frac{\partial u}{\partial x}+\frac{\partial v}{\partial y}=0 \tag{1}$$

$$u\frac{\partial u}{\partial x}+v\frac{\partial u}{\partial y}=\frac{\mu_{hnf}}{\rho_{hnf}}\frac{\partial^2 y}{\partial y^2}+\beta_{hnf}\,g(T-T_\infty)-\frac{\sigma_{hnf}B_0^2 u}{\rho_{hnf}} \tag{2}$$

$$u\frac{\partial T}{\partial x}+v\frac{\partial T}{\partial y}=\frac{k_{hnf}}{(\rho C_P)_{hnf}}\frac{\partial^2 y}{\partial y^2}+\frac{1}{(\rho C_P)_{hnf}}\frac{\partial q_r}{\partial y} \tag{3}$$

Subject to the following boundary conditions:

$$u = U_w(x), \quad v = 0, \quad T = T_w(x), \quad at \ y = 0 \tag{4}$$

$$u \longrightarrow 0, \quad T \longrightarrow T_\infty, \ as \ y \longrightarrow \infty \tag{5}$$

Here, (u) and (v) represents the velocities in the (x) and (y) directions respectively, $(\rho C_p)_{hnf}$ denotes heat capacitance of the hybrid nanofluid, σ_{hnf} is the electrical conductivity of the hybrid nanofluid, T represents the local temperature of the fluid, T_∞ free stream temperature, T_w Surface temperature, U_w fluid velocity at the wall, k_{hnf} thermal conductivity of the hybrid nanofluid, ρ_{hnf} density of the hybrid nanofluid, μ_{hnf} represents dynamic viscosity of the hybrid nanofluid, β_{hnf} the coefficient of thermal expansion for the hybrid nanofluid and q_r is the the Rosseland approximation as given by Makinde and Eegunjobi (2016), $q_r = \frac{4\sigma^*}{3k^*}\frac{\partial T^4}{\partial y}$. The expression T^4 may be approximated as a linear function of the local temperature T. Employing a truncated expansion of the Taylor series around the free-stream temperature T_∞, we have the following approximation: $T^4 \cong 4TT_\infty^3 - 3T_\infty^4$.

The thermo-physical properties of hybrid nanofluids (Alharbi et al., 2019) are stated as follows

$$\rho_{hnf} = \{(1-\phi_2)[(1-\phi_1)\rho_f + \phi_1\rho s_1]\} + \phi_2\rho s_2 \tag{6}$$

$$\mu_{hnf} = \frac{\mu_f}{(1-\phi_1)^{2.5}(1-\phi_2)^{2.5}} \tag{7}$$

$$\frac{k_{hnf}}{k_f} = \left\{\frac{(1+2\phi)(\phi_1K_1+\phi_1K_1)+2(1-\phi)\phi k_f}{(1-\phi)(\phi_1K_1+\phi_1K_1)+(2+\phi)\phi k_f}\right\} \tag{8}$$

$$\frac{(\rho C_P)_{hnf}}{(\rho C_P)_f} = \left\{(1-\phi) + \phi_1\frac{(\rho C_P)_1}{(\rho C_P)_f} + \phi_2\frac{(\rho C_P)_2}{(\rho C_P)_f}\right\} \tag{9}$$

$$\frac{\sigma_{hnf}}{\sigma_f} = 1 + \frac{\left(\frac{\phi_1\sigma_1+\phi_2\sigma_2}{\sigma_f}\right)-3(\phi_1+\phi_2)}{2+\left(\frac{\phi_1\sigma_1+\phi_2\sigma_2}{(\phi_1+\phi_2)\sigma_f}\right)-\left[\frac{\phi_1\sigma_1+\phi_2\sigma_2}{\sigma_f}-(\phi_1+\phi_2)\right]} \tag{10}$$

The similarity transforms used are:

$$\eta = y\left(\frac{a}{\nu_f}\right)^{\frac{1}{2}} \quad \psi = (a\nu_f)^{\frac{1}{2}}xf(\eta) \quad \theta(\eta) = \frac{T-T_\infty}{T_w-T_\infty}$$

$$A_1 = \frac{(1-\phi)^{2.5}}{\left(1-\phi+\phi_1\frac{\rho_1}{\rho_f}+\phi_2\frac{\rho_2}{\rho_f}\right)} \quad A_2 = \frac{\left\{\frac{(1+2\phi)(\phi_1K_1+\phi_1K_1)+2(1-\phi)\phi k_f}{(1-\phi)(\phi_1K_1+\phi_1K_1)+(2+\phi)\phi k_f}\right\}}{\left\{(1-\phi)+\phi_1\frac{(\rho C_P)_1}{(\rho C_P)_f}+\phi_2\frac{(\rho C_P)_2}{(\rho C_P)_f}\right\}} \quad \mathrm{Gr} = \frac{\beta_{hnf}g(T_w-T_\infty)}{a^2x}$$

$$\mathrm{M} = \frac{\sigma_{hnf}}{a\rho_{hnf}}B_0^2 \quad R = \frac{4\sigma^*T_\infty^3}{3k^*k_{hnf}} \quad pr = \frac{\nu_f}{\alpha_f} \quad \phi = \phi_1 + \phi_2 \tag{11}$$

Where, η is the similarity variable, θ is the dimensionless temperature, ϕ_1 and ϕ_2 are the volume fraction of copper and aluminum nanoparticles respectively and ψ is the stream function with the velocity terms given as;

$$u = \frac{\partial\psi}{\partial y} \quad v = -\frac{\partial\psi}{\partial x} \tag{12}$$

Substituting equation (10) into equation (1) - (5), hence, the dimensionless equations are given as follows;

$$A_1 f''' + Gr\theta - Mf' - (f')^2 + ff'' = 0$$

$$A_2\left(1+\frac{4}{3}R\right)\theta'' + prf\theta' = 0 \tag{13}$$

With the transformed boundary conditions

$$\text{At } \eta = 0, \quad f' = 1 \quad f = 0 \quad \theta = 1 \tag{14}$$

$$\text{As } \eta \longrightarrow \infty, \quad f' \longrightarrow 0 \quad \theta \longrightarrow 0 \tag{15}$$

Prime represents the differentiation with respect to η, Gr is the Buoyancy parameter arising from similarity transformation, M is the Magnetic parameter, A_1 and A_2 represent the thermophysical properties of hybrid nanofluid, R Radiation parameter, and Pr is the Prandtl number.

Quantitative Measures

Fluid flow resistance and heat transfer efficiency are evaluated using two essential indicators: the local skin friction coefficient (C_f) and the Nusselt number (Nu_x).

$$C_f = \frac{\tau_w}{\rho_f U_w^2} = \frac{\mu_{hnf}}{\rho_f U_w^2}\left(\frac{\partial u}{\partial y}\right)_{y=0}$$

$$Nu_x = \frac{x q_w}{k_f(T_w - T_\infty)} = -k_{hnf}\frac{x\left(\frac{\partial T}{\partial y}\right)_{y=0}}{(T_w - T_\infty)} \tag{16}$$

Using the similarity transform in equations (11) and (16) we get the following terms:

$$(Re_x)^{\frac{1}{2}} C_f = \frac{\mu_{hnf}}{\mu_f} f''(0)$$

$$(Re_x)^{\frac{-1}{2}} Nu_x = -\frac{k_{hnf}}{k_f}\theta'(0) \tag{17}$$

Where $Re_x = \frac{U_w(x)x}{v_f} = \frac{ax^2}{v_f}$, $\tau_w = \mu_{hnf}\left(\frac{\partial u}{\partial y}\right)_{y=0}$, $q_w = -k_{hnf}\left(\frac{\partial T}{\partial y}\right)_{y=0}$

Entropy Generation Analysis

Entropy generation analysis is employed to quantify thermodynamic irreversibility in the present MHD hybrid nanofluid flow. The total entropy arises from heat transfer, viscous dissipation, and magnetic effects within the boundary layer.

$$E_G = \frac{1}{T_\infty^2}\left[\frac{K_{hnf}}{k_f} + \frac{16\sigma^* T_\infty^3}{3k^* k_f}\right]\left(\frac{\partial T}{\partial y}\right)^2 + \frac{\mu_{hnf}}{T_\infty}\left(\frac{\partial u}{\partial y}\right)^2 + \frac{\sigma_{hnf} B_0^2}{T_\infty} u^2 \tag{18}$$

The first term represents entropy generation associated with heat transfer, including the effects of thermal radiation. The second term accounts for entropy production due to viscous dissipation within the fluid. The third term describes entropy generation arising from the influence of the magnetic field.

The entropy generation number in its non-dimensional form is defined as follows

$$E_{G0} = \frac{T_\infty^2}{k_f(T_W - T_\infty)^2}\frac{v_f}{a}E_G$$

Under the similarity transformations defined in Equation (11), the entropy generation expression is converted into its corresponding non-dimensional form.

$$N_S = \left[\frac{k_{hnf}}{k_f} + Rd\right]\theta'^2 + \frac{Br}{\Omega}\left[\frac{\mu_{hnf}}{\mu_f}f''^2 + M\frac{\sigma_{hnf}}{\sigma_f}f'^2\right] \quad (19)$$

Here, the Brinkman number is defined as $Br = \frac{\mu_f a^2 x^2}{k_f(T_w - T_\infty)}$ which characterizes the relative contribution of viscous heating within the boundary layer compared to heat conduction from the surface. The parameter Ω is given by $\Omega = \frac{T_w - T_\infty}{T_\infty}$ and represents the non-dimensional temperature difference between the surface and the ambient fluid.

N_S which is the total entropy of the system, can be written as the sum of N_1 which is the the entropy number due to thermal effect with thermal radiation N_2 on the other hand is the entropy number due to fluid friction and magnetic fields given as

$$N_1 = \left[\frac{k_{hnf}}{k_f} + Rd\right]\theta'^2 \quad N_2 = \frac{Br}{\Omega}\left[\frac{\mu_{hnf}}{\mu_f}f''^2 + M\frac{\sigma_{hnf}}{\sigma_f}f'^2\right]$$

The Bejan number is defined as the ratio of entropy generation due to heat transfer to the total entropy generation arising from heat transfer, fluid friction, and magnetic effects (Bejan & Kestin, 1983). Based on the present entropy generation model, it is expressed as

$$Be = \frac{Entropy\ due\ to\ heat\ transfer}{Total\ entropy\ generation} = \frac{N_1}{N_s}$$

and is evaluated locally within the boundary layer to characterise the dominant irreversibility mechanism.

Numerical solutions

The boundary layer equations were solved numerically using the shooting technique combined with the fourth-order Runge–Kutta method implemented in MATLAB. The boundary value problem was first transformed into an equivalent initial value problem by introducing unknown initial conditions, which were iteratively adjusted to satisfy the boundary conditions at infinity.

The numerical method was adopted due to its simplicity, accuracy, and effectiveness in handling nonlinear boundary layer problems through the transformation of boundary value problems into initial value problems. However, the method is sensitive to initial guesses, which may influence convergence speed or lead to divergence if poorly chosen, and it may become less efficient for highly stiff or large systems.

Convergence was achieved using a tolerance level of 10^{-5}, ensuring that successive iterations of the velocity and temperature profiles differed negligibly. The accuracy of the numerical results was further confirmed by refining the step size and verifying the stability of key physical quantities such as the skin friction coefficient and Nusselt number, which showed negligible variation across iterations.

Setting

$$p_1 = f, \quad p_2 = f', \quad p_3 = f'', \quad p_4 = \theta, \quad p_5 = \theta' \quad (20)$$

The boundary conditions (13) and (14) are converted to initial conditions as follows

$$p_1(0) = 0, \quad p_2(0) = 1, \quad p_3(0) = r_1, \quad p_4(0) = 1, \quad p_5(0) = r_2 \tag{21}$$

The emerging Initial Value problems of the differential first-order equations are given as follows:

$$p_1' = p_2 \tag{22}$$

$$p_2' = p_3 \tag{23}$$

$$p_3' = \frac{1}{A_1}(MP_2 + p_2^2 - Grp_4 - p_1p_3) \tag{24}$$

$$p_4' = p_5 \tag{25}$$

$$p_5' = -\left(A_2\left(1 + \frac{4}{3}R\right)\right)^{-1}(Prp_1p_5) \tag{26}$$

Governed by the specified boundary condition

$$p_1(0) = 0, \quad p_2(0) = 1, \quad p_3(0) = r_1, p_4(0) = 1, \quad p_5(0) = r_2 \tag{27}$$

The undefined initial approximations r_1 and r_2 are presumed. The system of equations from (22) to (26) is solved with the undefined initial conditions r_1 and r_2. The results are then compared with the boundary conditions (14) and (15). If there is a variation, the process is repeated until improved values are arrived at.

Code Validation

To verify the reliability of the present numerical scheme, validation was performed for the classical case of regular fluids without nanoparticles. Table 1 presents the comparison of the computed surface heat transfer rate, expressed as $-\theta'(0)$, across different Prandtl numbers. The results obtained in this study show very close agreement with those reported previously by Nandy et al. (2025). This consistency throughout the range of Pr considered confirms the accuracy of the numerical procedure and highlights the robustness of the mathematical model adopted in the current analysis.

Table 1: Comparative results of $-\theta'(0)$ when M = 0, R = 0, $\phi_1 = \phi_2 = 0$ for different values of the Prandtl number (Pr)

Pr	Nandy et al. (2025)	Present
0.70	0.453907	0.45445
2.00	0.911424	0.91135
7.00	1.835427	1.8954

Results and Discussions

Here, the following parameters: (Gr) buoyancy parameter, (Pr) Prandtl number, (R) Radiation parameter, (ϕ) Volume fraction, and *(M)* Magnetic parameter are discussed. The thermo-physical properties of the nanoparticles with the base fluid are given in Table 2. The skin friction coefficient and Nusselt number, which quantify wall shear and heat transfer respectively, are computed and presented in Table 3. For the baseline case, the values are set as *Gr* = 1, *M* =1, *R* =3, *Pr* =4, $\phi_1 = \phi_2 = 0.02$.

Table 2: Thermo-physical characteristics of the nanoparticles (Alharbi et al., 2019) and the base fluid (Krishna et al., 2021)

Materials	Density $(p)(kgm^{-3})$	Specific heat $(c_p)(jkgk^{-1})$	Thermal conductivity $(K_1)(wmk^{-1})$	Electrical conductivity $\sigma(\Omega/m)$
Copper	8933	385	400	5.96×10^{7}
Aluminium Oxide	3970	765	40	3.69×10^{7}
Water	997.1	4179	0.613	5.5×10^{-6}

Primary velocity profile

The influence of key parameters on the primary velocity of the hybrid nanofluid is illustrated in Figures 2–5. Figure 2 shows that increasing the buoyancy parameter enhances fluid motion, as buoyancy forces dominate over viscous resistance. This results in a thicker velocity boundary layer and higher velocity values near the wall, with the profiles approaching the free-stream asymptote more gradually. In Figure 3, increasing the magnetic parameter introduces stronger Lorentz forces, which act as a resistive mechanism against fluid motion. Consequently, the velocity boundary layer becomes thinner, the slope near the wall decreases, and the profiles decay more rapidly toward the asymptotic free-stream condition. Figure 4 demonstrates the effect of the Prandtl number: larger Pr values reduce thermal diffusivity, which indirectly alters the coupling between thermal and momentum layers. The velocity boundary layer contracts, and the slope at the wall steepens, indicating stronger shear effects. Finally, Figure 5 highlights the role of radiation. Higher radiation elevates the fluid temperature, which modifies the energy distribution and shifts the velocity boundary layer upward. This produces a thicker velocity profile with noticeable slope changes near the wall.

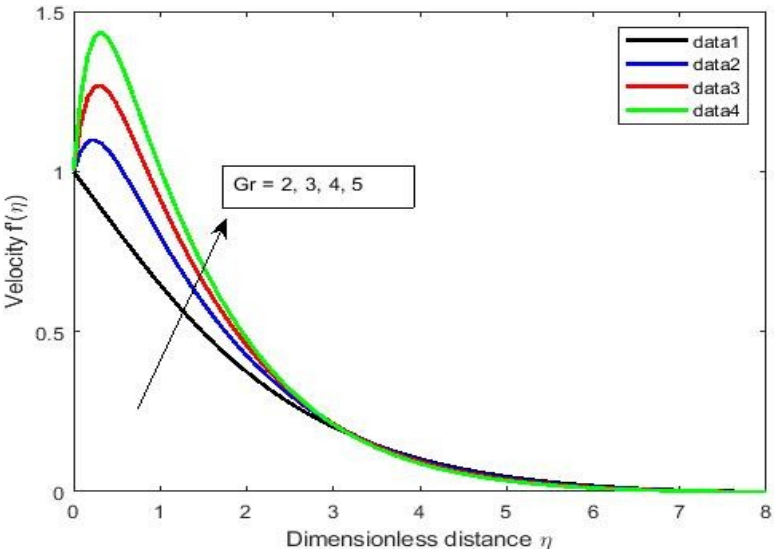

Figure 2: Variation of primary velocity with buoyancy parameter

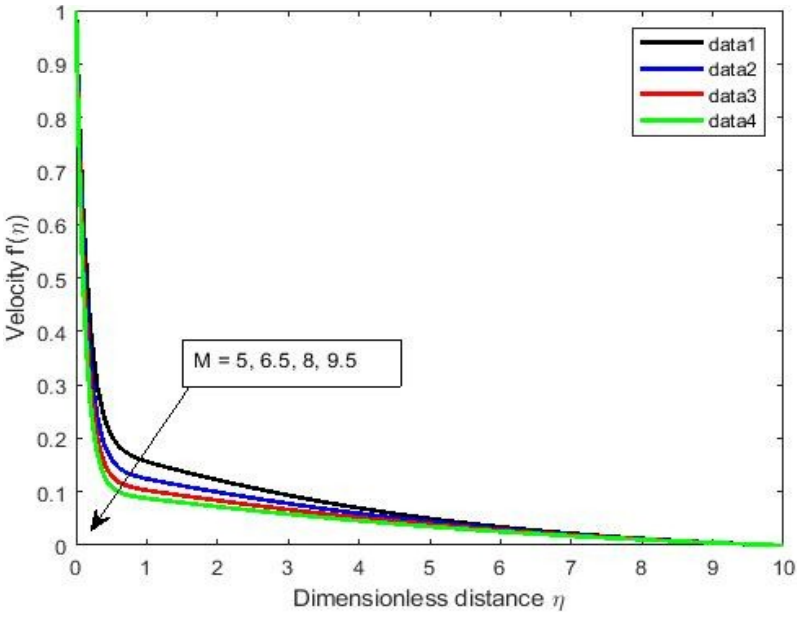

Figure 3: Variation of primary velocity with magnetic parameter

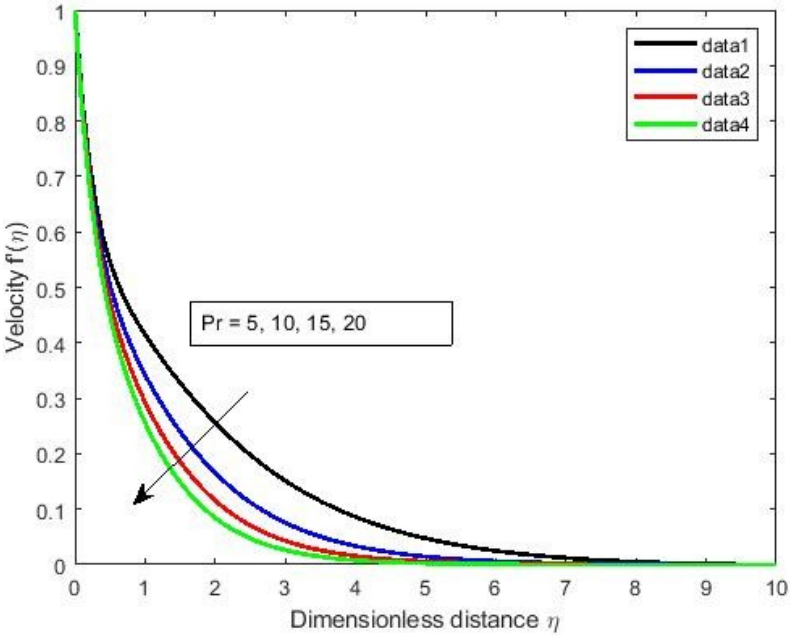

Figure 4: Variation of primary velocity with Prandtl number

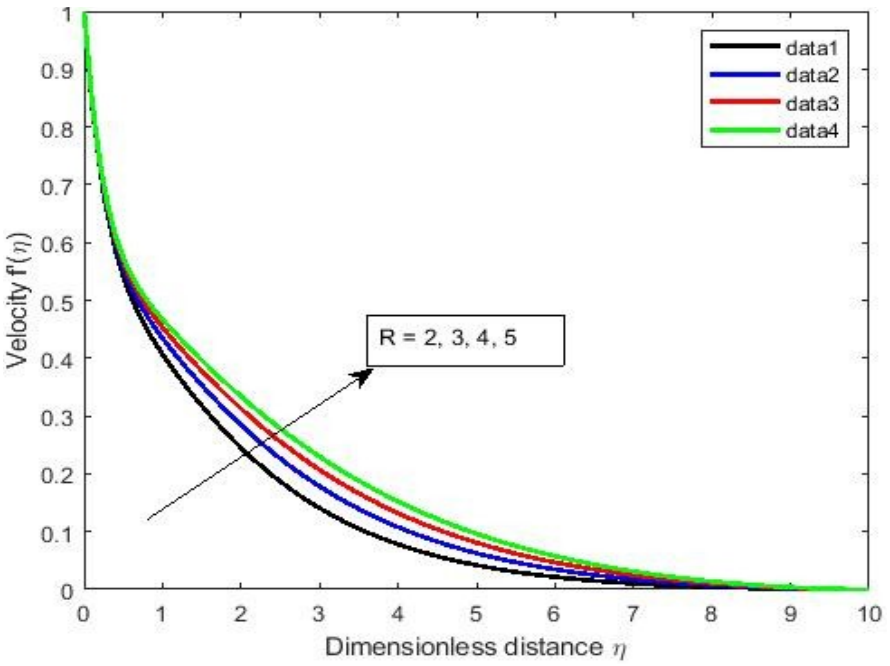

Figure 5: Variation of primary velocity with radiation parameter

Temperature profile

Figures 6–10 illustrate the effect of governing parameters on the temperature distribution of the hybrid nanofluid. Figure 6 shows that increasing the buoyancy parameter reduces the temperature profile, as stronger convection enhances heat transfer and thins the thermal boundary layer. This leads to a steeper wall temperature gradient and faster decay of the profile toward the ambient condition. In Figure 7, intensifying the magnetic parameter increases the temperature distribution. The Lorentz force resists fluid motion, which suppresses convective transport and thickens the thermal boundary layer, resulting in higher fluid temperatures near the wall. Figure 8 demonstrates that raising the nanoparticle volume fraction improves thermal conductivity, thereby elevating the temperature throughout the flow and producing a thicker thermal boundary layer. Figure 9 highlights the role of the Prandtl number: larger Pr values reduce thermal diffusivity, which contracts the thermal boundary layer and lowers the temperature profile, consistent with stronger wall gradients. Finally, Figure 10 shows that radiation increases the temperature distribution. Radiative heating elevates the fluid temperature close to the surface, thickening the thermal boundary layer and reducing the slope at the wall.

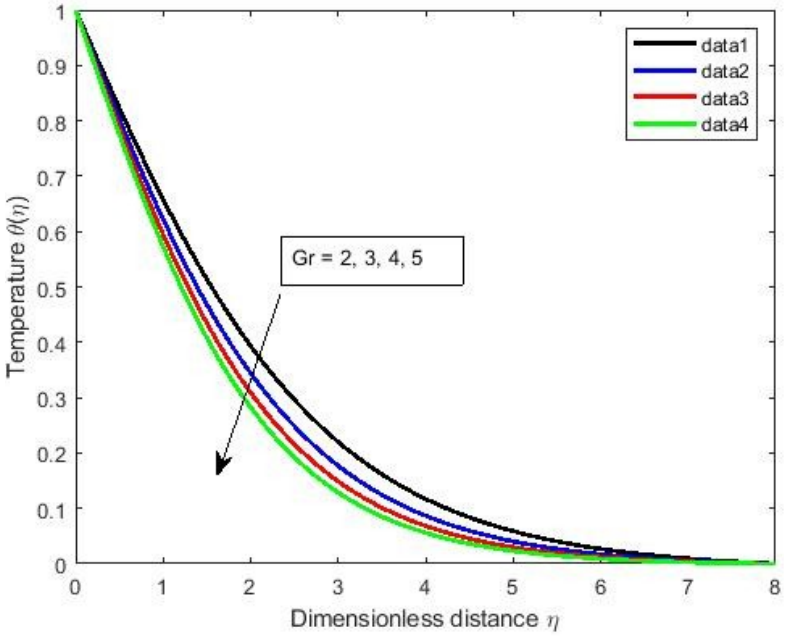

Figure 6: Variation of temperature with buoyancy parameter

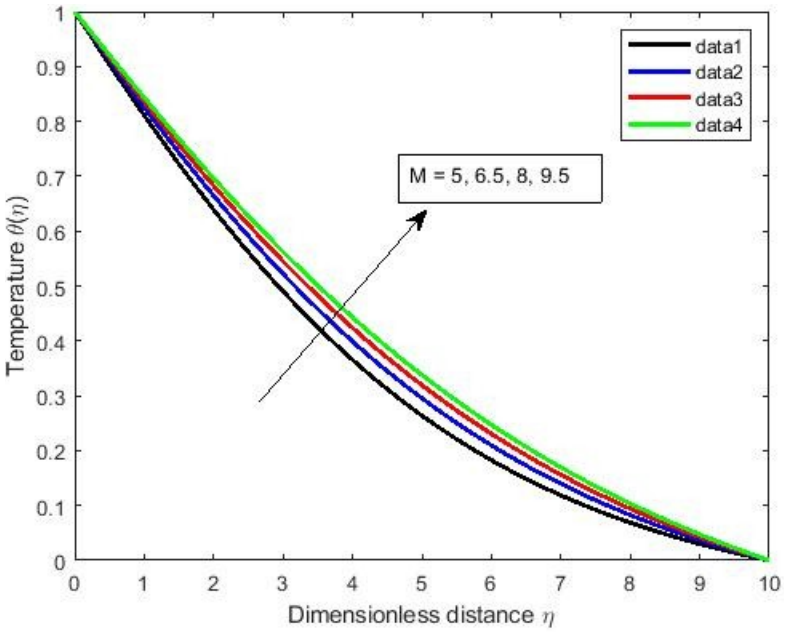

Figure 7: Variation of temperature with magnetic parameter

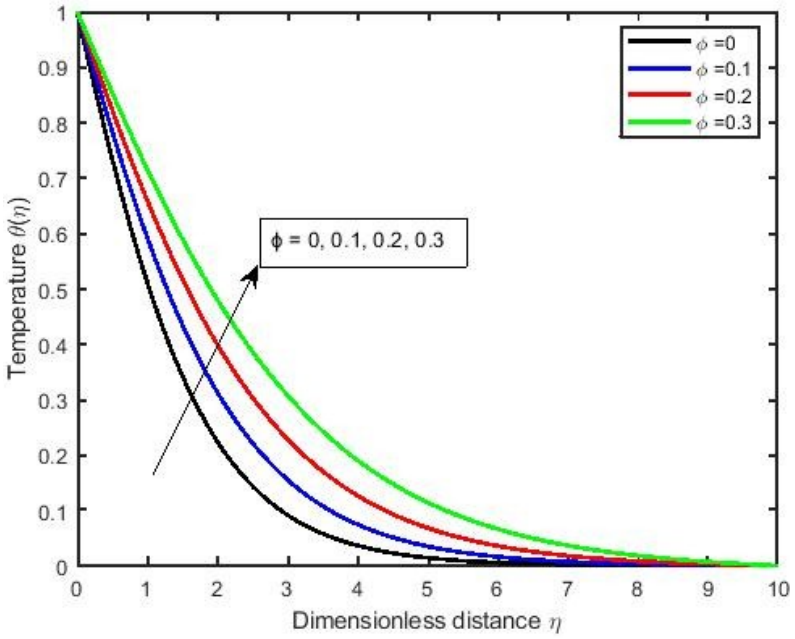

Figure 8: Variation of temperature with volume fraction

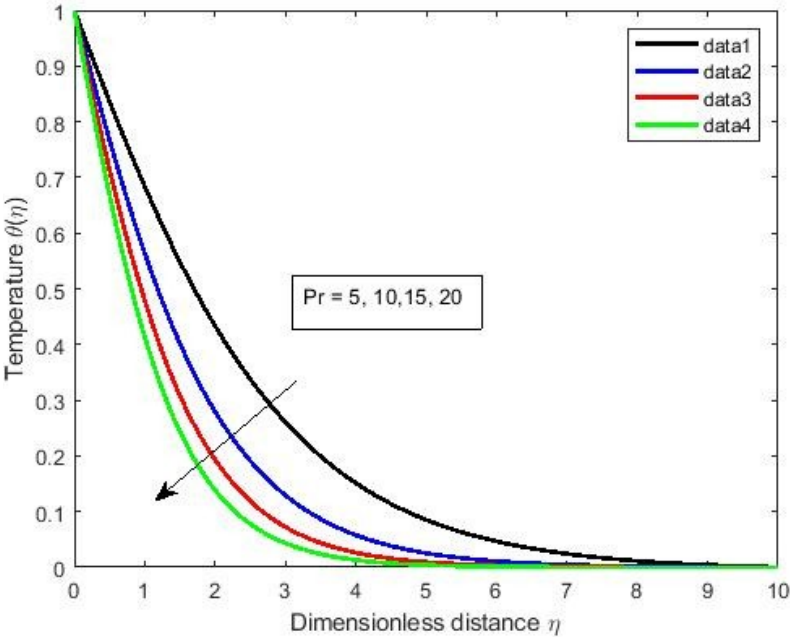

Figure 9: Variation of temperature with Prandtl number

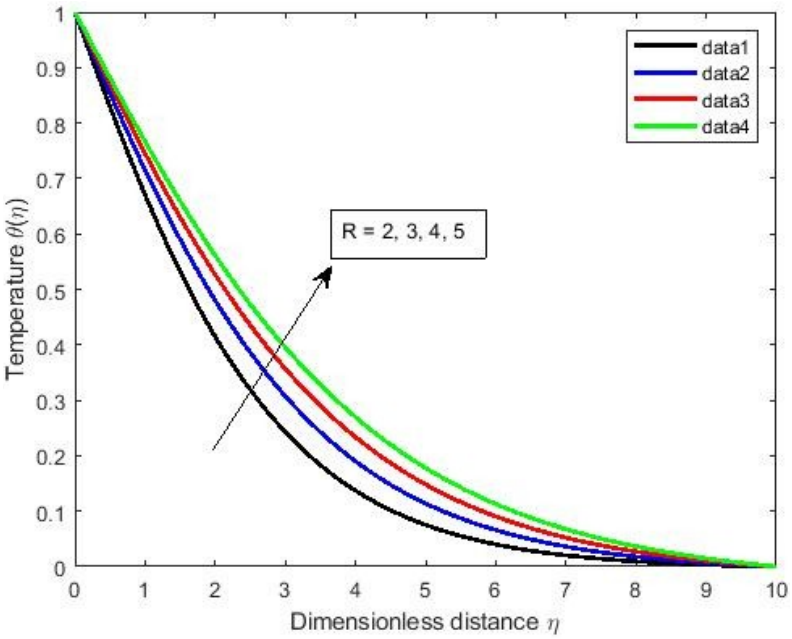

Figure 10: Variation of temperature with radiation parameter

Quantitative Measures

As evident in Table 3, increasing the buoyancy parameter enhances both skin friction and Nusselt number, reflecting buoyancy-driven convection. In contrast, a stronger magnetic field reduces skin friction and Nusselt number, consistent with Lorentz damping effects. Raising the Prandtl number increases Nusselt number while reducing skin friction, highlighting the role of reduced thermal diffusivity in strengthening heat transfer. Radiation shows mixed behaviour, decreasing Nusselt number but increasing skin friction, as radiative heating elevates the fluid temperature profile while weakening the wall gradient.

Table 3: Variation of skin friction coefficient and Nusselt number with governing parameters

Gr	M	R	Pr	$(Re_x)^{\frac{1}{2}}C_f$	$(Re_x)^{\frac{-1}{2}}Nu_x$	$(Re_x)^{\frac{1}{2}}C_f$	$(Re_x)^{\frac{-1}{2}}Nu_x$
2 3 4 5	1	3	4	-0.000537276 0.0000119822 0.000531477 0.001028781	0.597828886 0.644003468 0.680692058 0.711533372	↑	↑
1	5 6.5 8 9.5	3	4	-0.00267601 -0.003090402 -0.003459725 -0.003795599	0.381851344 0.351662353 0.328255337 0.309539678	↓	↓
1	1	3.5 4 5 6	4	-0.001116071 -0.00110294 -0.001081594 -0.001064881	0.496275139 0.466148977 0.419030167 0.383621411	↑	↓
1	1	3	6 8 10 12	-0.001185338 -0.00122683 -0.001260398 -0.001288419	0.672233354 0.794407048 0.904933486 1.006814437	↓	↑

Entropy Generation and Bejan Number Analysis

Entropy generation and Bejan number were evaluated to capture the thermodynamic behaviour of the hybrid nanofluid under varying parameters. In all cases, entropy generation peaks near the wall and decays toward the free stream, while the Bejan number rises from near zero to values approaching unity, marking the shift from viscous-dominated to heat-transfer-dominated irreversibility. In Figure 11a, increasing the magnetic parameter (M) elevates entropy generation because Lorentz forces resist fluid motion and intensify viscous dissipation. The corresponding Figure 11b shows the Bejan number decreasing, reflecting the dominance of viscous irreversibility. Similarly, Figures 12a and 12b demonstrate that a higher Brinkman number (Br) raises entropy generation and lowers the Bejan number, confirming that viscous heating amplifies total irreversibility. By contrast, Figures 13a and 13b reveal that increasing the temperature-difference parameter (Ω) reduces entropy generation and enhances the Bejan number, as weaker temperature gradients diminish viscous effects and improve thermodynamic efficiency. Finally, Figures 14a and 14b indicate that the radiation parameter (R) increases both entropy generation and Bejan number, showing that radiative heat transfer elevates thermal energy and strengthens heat-transfer irreversibility. Across all cases, Cu–water produces the highest entropy generation, the hybrid Cu–Al_2O_3/water nanofluid lies in between, and Al_2O_3–water yields the lowest. This ordering reflects differences in thermal conductivity and viscosity. Overall, the hybrid nanofluid achieves a balanced outcome, enhancing heat transfer while moderating entropy production, highlighting its advantage in optimising energy utilisation under magnetohydrodynamic and radiative conditions.

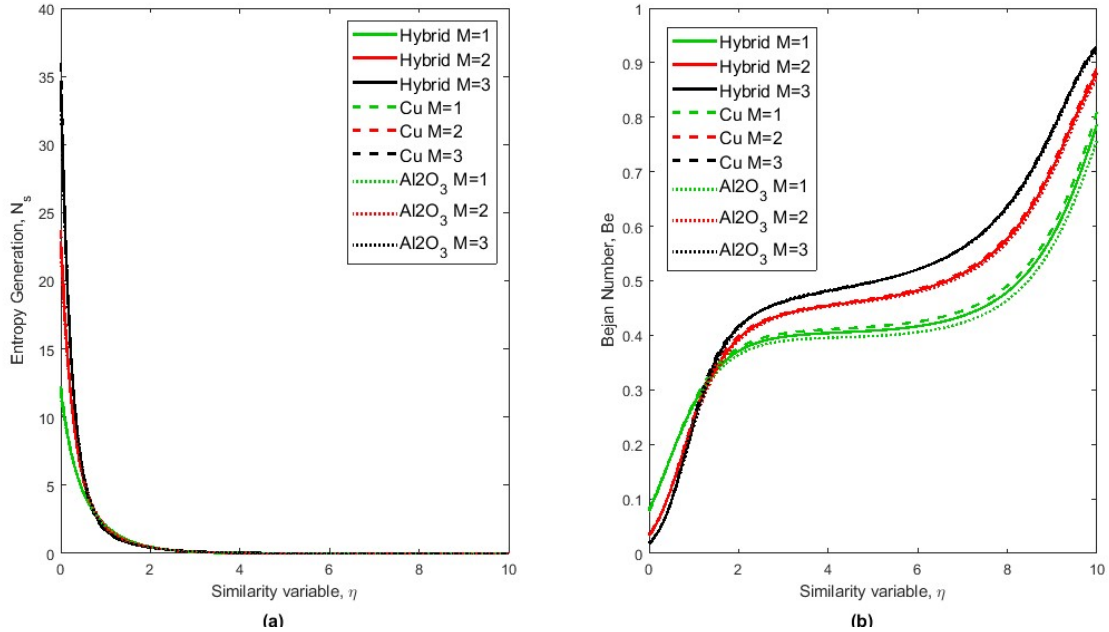

Figure 11: Variation of entropy generation (a) and Bejan number (b) with magnetic parameter (M)

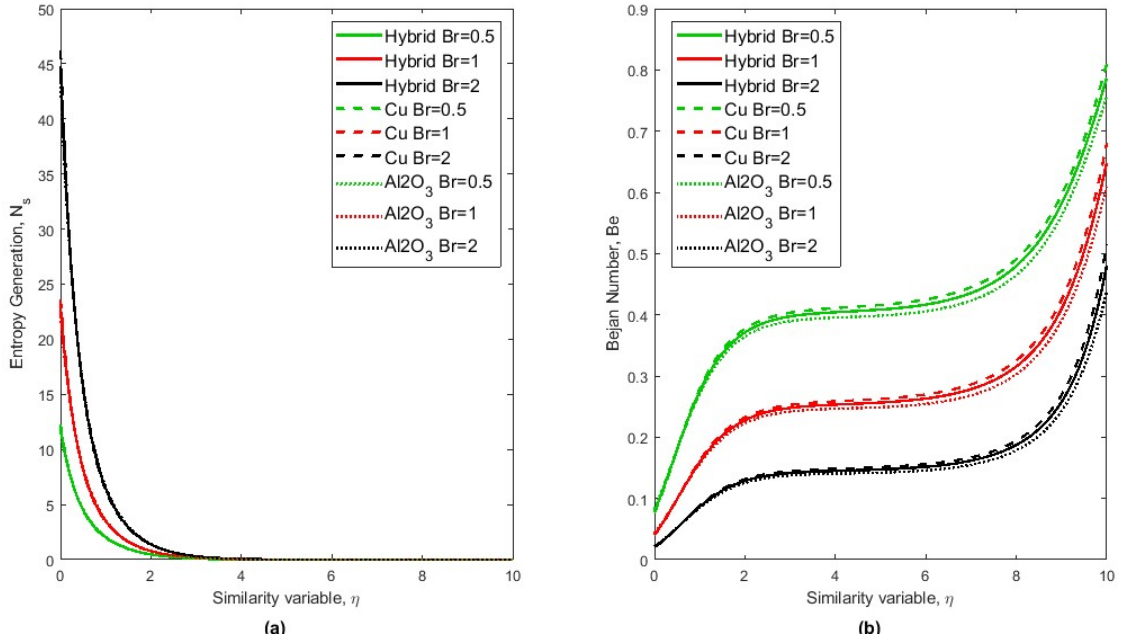

Figure 12: Variation of entropy generation (a) and Bejan number (b) with Brinkman number (Br)

Journal of Science, Innovation and Creativity
Vol. 5 No. 1 (2026): ISSN (Online): 2958-454X
DOI: https://doi.org/10.58721/jsic.v5i1.1705
Numerical Analysis of Magnetohydrodynamics Hybrid Nanofluid Flow Past an Infinite Vertical Plate in Presence of Thermal Radiation

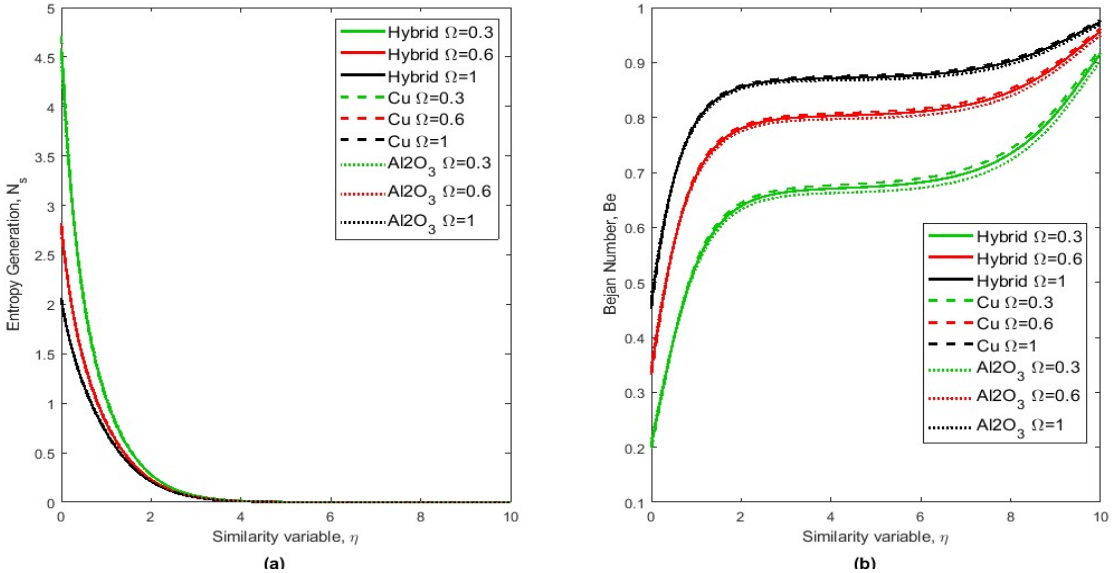

Figure 13: Variation of entropy generation (a) and Bejan number (b) with temperature-difference parameter (Ω).

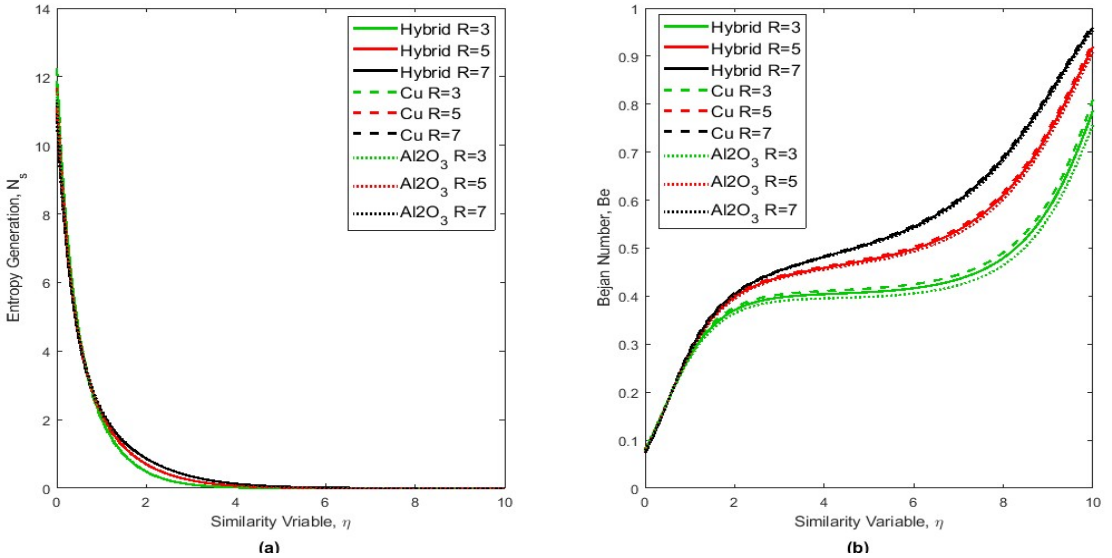

Figure 14: Variation of entropy generation (a) and Bejan number (b) with radiation parameter (R)

Conclusion

This study examined how magnetic fields, thermal radiation, and nanoparticle volume fraction influence the flow and heat transfer of a hybrid nanofluid across an infinitely vertical plate. The governing equations were formulated with appropriate boundary conditions, non-dimensionalised using similarity variables, and solved numerically via the shooting technique combined with the fourth-order Runge–Kutta method in MATLAB. The analysis presented velocity and temperature distributions, skin friction coefficient, Nusselt number, entropy generation, and Bejan number under varying physical parameters.

The findings include:

- An increase in the buoyancy parameter and radiation parameter enhances the primary velocity, whereas a higher Prandtl number and magnetic parameter lead to its reduction.
- The temperature distribution decreases with buoyancy forces and Prandtl number, but increases with magnetic parameter, volume fraction and Radiation parameter.
- The hybrid nanofluid's thermal performance and heat transmission are improved by raising thermal radiation and the volume fractions of the nanoparticles.
- Skin friction coefficient rises with intensifying buoyancy forces and radiation parameter but declines with magnetic fields and Prandtl number.
- The Nusselt number increases with increasing buoyancy forces and the Prandtl number, but decreases with increasing radiation and magnetic field strength.
- Entropy generation increases with magnetic and Brinkman numbers due to viscous dissipation, decreases with the temperature-difference parameter, and rises again with radiation.
- Bejan number transitions from near zero to values approaching unity, indicating a shift from viscous-dominated to heat-transfer-dominated irreversibility. It decreases with the magnetic and Brinkman numbers, increases with the temperature-difference parameter, and also increases with radiation.
- Among the fluids studied, Cu–water exhibits the highest entropy generation, Al_2O_3–water the lowest, and the hybrid Cu–Al_2O_3/water nanofluid maintains intermediate values, reflecting its balanced thermal conductivity and viscosity.

The hybrid nanofluid demonstrates a favourable balance: it enhances heat transfer while moderating entropy production, underscoring its potential for efficient energy utilisation in magnetohydrodynamic and radiative environments. While the present analysis captures clear trends, it assumes uniform nanoparticle dispersion and simplified boundary conditions. Future work should incorporate three-dimensional, unsteady flow, porous effect, and convective instabilities to extend the scope and applicability of hybrid nanofluids in engineering systems.

References

Alharbi, S. O., Nawaz, M., & Nazir, U. (2019). Thermal analysis for hybrid nanofluid past a cylinder exposed to magnetic field. *AIP Advances, 9*(11). https://doi.org/10.1063/1.5127327

Amran, M. F., Sultan, S. M., & Tso, C. P. (2024). A comprehensive review of mixed convective heat transfer in tubes and ducts: Effects of Prandtl number, geometry, and orientation. *Processes*, *12*(12), 2749. https://doi.org/10.3390/pr12122749

Anantha Kumar, K., Sugunamma, V., & Sandeep, N. (2020). Effect of thermal radiation on MHD Casson fluid flow over an exponentially stretching curved sheet. *Journal of Thermal Analysis and Calorimetry*, 140, 2377-2385. https://doi.org/10.1007/s10973-019-08977-0

Bejan, A., & Kestin, J. (1983). Entropy generation through heat and fluid flow.

Choi, S. U., & Eastman, J. A. (1995). Enhancing thermal conductivity of fluids with nanoparticles (No. ANL/MSD/CP-84938; CONF-951135-29). Argonne National Lab. (ANL), Argonne, IL (United States).

Daniel, Y. S., Aziz, Z. A., Ismail, Z., & Salah, F. (2017). Effects of thermal radiation, viscous and Joule heating on electrical MHD nanofluid with double stratification. *Chinese Journal of Physics, 55*(3), 630-651. https://doi.org/10.1016/j.cjph.2017.04.001

Daniel, Y. S., Aziz, Z. A., Ismail, Z., & Salah, F. (2019). Thermal radiation on unsteady electrical MHD flow of nanofluid over stretching sheet with chemical reaction. *Journal of King Saud University-Science, 31*(4), 804-812. https://doi.org/10.1016/j.jksus.2017.10.002

Hafeez, A., Liu, D., & Khalid, A. (2025). MHD flow of radiative hybrid nanofluid across a wedge influenced by melting heat transfer: engineering application. *Alexandria Engineering Journal*, *122*, 18-27.https://doi.org/10.1016/j.aej.2025.03.018

Hayat, T., & Nadeem, S. (2017). Heat transfer enhancement with Ag–CuO/water hybrid nanofluid. Results in physics, 7, 2317-2324. https://doi.org/10.1016/j.rinp.2017.06.034

Khalatbari, S., Jalili, P., Jalili, B., & Ganji, D. D. (2025). Investigating the improvement of heat transfer and flow characteristics of hybrid nanofluids: A comprehensive review. *Proceedings of the Institution of Mechanical Engineers, Part E: Journal of Process Mechanical Engineering*, 09544089251318785. https://doi.org/10.1177/09544089251318785

Krishna, M. V., Ahammad, N. A., & Chamkha, A. J. (2021). Radiative MHD flow of Casson hybrid nanofluid over an infinite exponentially accelerated vertical porous surface. *Case Studies in Thermal Engineering, 27*, 101229. https://doi.org/10.1016/j.csite.2021.101229

Mahdy, A., El-Zahar, E. R., Rashad, A. M., Saad, W., & Al-Juaydi, H. S. (2021). The magneto-natural convection flow of a micropolar hybrid nanofluid over a vertical plate saturated in a porous medium. *Fluids, 6*(6), 202. https://doi.org/10.3390/fluids6060202

Manimaran, M., Norizan, M. N., Kassim, M. H. M., Adam, M. R., Abdullah, N., & Norrrahim, M. N. F. (2025). Critical review on the stability and thermal conductivity of water-based hybrid nanofluids for heat transfer applications. *RSC advances*, *15*(18), 14088-14125. https://doi.org/10.1039/D5RA00844A

Maxwell, J. C. (1873). *A treatise on electricity and magnetism (Vol. 1)*. Clarendon Press.

Mohanty, B., Mishra, S. R., & Pattanayak, H. B. (2015). Numerical investigation on heat and mass transfer effect of micropolar fluid over a stretching sheet through porous media. *Alexandria Engineering Journal, 54*(2), 223-232. https://doi.org/10.1016/j.aej.2015.03.010

Molla, M. M., Hasan, M. F., & Islam, M. M. (2025). Elucidating thermal phenomena of non-Newtonian experimental data based copper-alumina-ethylene glycol hybrid nanofluid in a cubic enclosure with central heated plate by machine learning validations of D3Q27 MRT-LBM. *International Journal of Thermofluids*, *26*, 101033.https://doi.org/10.1016/j.ijft.2024.101033

Murugan, R. D., Sivakumar, N., Tarakaramu, N., Ahmad, H., & Askar, S. (2024). Entropy generation on MHD motion of hybrid nanofluid with porous medium in presence of thermo-radiation and ohmic viscous dissipation. *Discover Applied Sciences*, *6*(4), 199. https://doi.org/10.1007/s42452-024-05866-6

Nandy, S. K., Mandal, R. K., & Mondal, S. (2025). Magneto-radiative slip flow of couple stress Cu–Al_2O_3 hybrid nanofluid over a stretching sheet with activation energy. *Journal of Advanced Thermal Science Research*, *12*, 170-193.https://doi.org/10.15377/2409-5826.2025.12.10

Nath, R. S., & Deka, R. K. (2024). Theoretical study of thermal and mass stratification effects on MHD nanofluid past an exponentially accelerated vertical plate in a porous medium in presence of heat source, thermal radiation and chemical reaction. *International Journal of Applied and Computational Mathematics, 10*(2), 92. https://doi.org/10.1007/s40819-024-01721-9

Nayak, M. K., Akbar, N. S., Pandey, V. S., Khan, Z. H., & Tripathi, D. (2017). 3D free convective MHD flow of nanofluid over permeable linear stretching sheet with thermal radiation. *Powder Technology*, 315, 205-215. https://doi.org/10.1016/j.powtec.2017.04.017

Nayak, M. K., Pasha, A. A., Kamilla, B. S., Thatoi, D. N., Juhany, K., Kouki, M., ... & Galal, A. M. (2025). Synthesis, stability, and heat transfer applications of ternary composite nanofluids: A review over the last decade. *Results in Engineering*, *25*, 104284.https://doi.org/10.1016/j.rineng.2025.104284

Rajesh, V., & Chamkha, A. J. (2022). Impact of hybrid nanofluids on unsteady MHD flow and heat transfer due to a moving infinite vertical plate. *Heat Transfer, 51*(2), 1358-1375 . https://doi.org/10.1002/htj.22355

Rangra, N., Arslan, M. S., Abbas, Z., & Rafiq, M. Y. (2025). Entropy generation analysis in MHD hybrid nanofluid flow over a rotating surface for sustainable energy applications. *Results in Engineering*, 106765. https://doi.org/10.1016/j.rineng.2025.106765

Reddy, Y. D., & Goud, B. S. (2023). Comprehensive analysis of thermal radiation impact on an unsteady MHD nanofluid flow across an infinite vertical flat plate with ramped temperature with heat consumption. *Results in Engineering, 17*, 100796.

Sharma, P., Sharma, B. K., Gandhi, R., Almohsen, B., & Pérez, L. M. (2024). Computational analysis of entropy generation optimisation for Cu–Al2O3 water-based chemically reactive magnetised radiative hybrid nanofluid flow. *AIP Advances*, *14*(7). https://doi.org/10.1063/5.0213946

Sheikholeslami, M., Ganji, D. D., Javed, M. Y., & Ellahi, R. (2015). Effect of thermal radiation on magnetohydrodynamics nanofluid flow and heat transfer by means of two-phase model. *Journal of magnetism and Magnetic materials*, 374, 36-43. https://doi.org/10.1016/j.jmmm.2014.08.021

Shoaib, M., Raja, M. A. Z., Sabir, M. T., Islam, S., Shah, Z., Kumam, P., & Alrabaiah, H. (2020). Numerical investigation for rotating flow of MHD hybrid nanofluid with thermal radiation over a stretching sheet. *Scientific Reports, 10*(1), 18533. https://doi.org/10.1038/s41598-020-75254-8

Suresh Kumar, Y., Hussain, S., Raghunath, K., Ali, F., Guedri, K., Eldin, S. M., & Khan, M. I. (2023). Numerical analysis of magnetohydrodynamics Casson nanofluid flow with activation energy, Hall current and thermal radiation. *Scientific Reports, 13*(1), 4021. https://doi.org/10.1038/s41598-023-28379-5

Ullah, H., Hayat, T., Ahmad, S., Alhodaly, M. S., & Momani, S. (2021). Numerical simulation of MHD hybrid nanofluid flow by a stretchable surface. *Chinese Journal of Physics, 71*, 597-609. https://doi.org/10.1016/j.cjph.2021.03.017

Waini, I., Ishak, A., & Pop, I. (2020b). Mixed convection flow over an exponentially stretching/shrinking vertical surface in a hybrid nanofluid. *Alexandria Engineering Journal*, *59*(3), 1881-1891.https://doi.org/10.1016/j.aej.2020.05.030

Waini, Iskandar, Anuar Ishak, & Ioan Pop. (2020a). Hybrid nanofluid flow induced by an exponentially shrinking sheet..*Chinese Journal of Physics, 68*, 468-482 https://doi.org/10.1016/j.cjph.2019.12.015

Xuan, Y. (2014). An overview of micro/nanoscaled thermal radiation and its applications. *Photonics and Nanostructures-Fundamentals and Applications, 12*(2),93-113.

Yashkun, U., Zaimi, K., Abu Bakar, N. A., Ishak, A., & Pop, I. (2021). MHD hybrid nanofluid flow over a permeable stretching/shrinking sheet with thermal radiation effect. *International Journal of Numerical Methods for Heat & Fluid Flow*, *31*(3), 1014-1031. https://doi.org/10.1108/HFF-02-2020-0083

Younes, H., Christensen, G., Li, D., Hong, H., & Ghaferi, A. A. (2015). Thermal conductivity of nanofluids. *Journal of Nanofluids, 4*(2), 107-132. https://doi.org/10.1166/jon.2015.1151